Cement and Concrete Research 40 (2010) 636–642

Contents lists available at ScienceDirect

Cement and Concrete Research

journal homepage: http://ees.elsevier.com/CEMCON/default.asp

Summary of research on the effect of $LiNO_3$ on alkali–silica reaction in new concrete

X. Feng [a], M.D.A. Thomas [a,*], T.W. Bremner [a], K.J. Folliard [b], B. Fournier [c]

[a] *Department of Civil Engineering, University of New Brunswick, Fredericton, NB, Canada*
[b] *Concrete Durability Center, the University of Texas at Austin, TX, USA*
[c] *Department of Geological Engineering, Laval University, Quebec, PQ, Canada*

ARTICLE INFO

Article history:
Received 27 November 2008
Accepted 19 August 2009

Keywords:
B SEM
B EDX
C Alkali-aggregate reaction
D Lithium compounds

ABSTRACT

This paper summarizes findings from a research study conducted at the University of New Brunswick in collaboration with the University of Texas at Austin, and CANMET-MTL, on the effect of $LiNO_3$ on ASR in new concrete. The studies included expansion testing, silica dissolution measurements and microstructural examinations of cement systems containing glass and two different reactive aggregates (NB and NS). Only a small proportion of the data are presented here for the purpose of highlighting the principal findings of this investigation.

Based on these findings, it is proposed that the inhibiting effect of $LiNO_3$ against ASR in new concrete is attributed to the formation of two reaction products in the presence of lithium, these being a crystalline lithium silicate compound (Li_2SiO_3) crystal and a Li-bearing, low Ca silica gel. These two phases could serve as a diffusion barrier and protective layer to prevent the reactive silica from further attack by alkalis.

It was found that the reason the two reactive aggregates selected responded differently to $LiNO_3$ was due to the difference in their textural features. The NB aggregate contained reactive volcanic glass particles, the surface of which was immediately and equally available to sodium, potassium and lithium, and thus a Li–Si barrier was able to form quickly. The reactive phase in the NS aggregate was microcrystalline and strained quartz, which was embedded in a dense matrix of a non-reactive predominantly alumino-silicate phase and was not easily accessible to lithium.

1. Introduction

The concept of using lithium compounds to mitigate the effects of ASR expansion was first reported by McCoy and Caldwell [1]. Since then, numerous research studies have been conducted to determine the effect and elucidate the mechanism of lithium compounds in controlling ASR-induced expansion [2–7]. A variety of lithium compounds including LiF, LiCl, LiBr, LiOH, $LiOH \cdot H_2O$, $LiNO_3$, $LiNO_2$, Li_2CO_3, Li_2SO_4, Li_2HPO_4, and Li_2SiO_3 have been used in these studies, but the most promising for suppressing the ASR expansion is $LiNO_3$ as it does not increase the hydroxyl ion concentration of the pore solution [8,9]. The benign effect of $LiNO_3$ on concrete properties, its neutrality and high solubility, have also favored the use of this material over other lithium compounds. Currently $LiNO_3$ additives are commercially available to control ASR, however, the inhibiting mechanism is still far from clear [10]. This paper presents a brief summary of some findings on the effect of $LiNO_3$ on ASR in new concrete from the ongoing research conducted at the University of New Brunswick as part of collaborative study with the University of Texas at Austin and CANMET-MTL in Ottawa.

2. Experimental studies

The work carried out in this research program on the effect of $LiNO_3$ on ASR in new concrete included the following studies:

- Expansion testing of mortar bars was in accordance with ASTM C 1260, concrete prisms in accordance with ASTM C 1293, and concrete microbars following the test method described by Grattan-Bellew [11], with two representative reactive coarse aggregates, were designated as NB and NS, respectively. NB is a rhyolite with 85% devitrified glass; NS is a greywacke with 8% microcrystalline quartz.
- Silica dissolution tests on NB and NS aggregates ground to a size between 150 μm and 300 μm. The aggregate powder was immersed in different alkaline solutions, with or without $LiNO_3$ at 100% standard Li dose (100% standard Li dose means a Li/Na molar ratio of 0.74), and in the presence or absence of $Ca(OH)_2$ at 80 °C. The amount of silica dissolved in the soaking solution and the changes in Li and Na ion concentrations in the solution were analyzed periodically by ICP-MS.
- Vycor glass disks and polished aggregate disks immersed in different alkaline solutions, with and without 0.74 M $LiNO_3$, and in the presence and absence of CH, and subsequent examinations by XRD and SEM. Data presented here are limited to specimens stored

---

* Corresponding author.
E-mail address: mdat@unb.ca (M.D.A. Thomas).

0008-8846/$ – see front matter © 2009 Elsevier Ltd. All rights reserved.
doi:10.1016/j.cemconres.2009.08.021

at 80 °C. Analysis of specimens stored at lower temperature (23 °C and 38 °C) are underway and will be reported is a subsequent paper.
- Vycor glass disk-cement paste specimen and polished aggregate disk-cement paste sandwich specimens were produced by placing a 5-mm thick layer of cement paste with [Li]/[Na + K] over the surface of a 5-mm thick sample of glass or polished aggregate. Specimens were immersed in 1 M NaOH + 0.74 M $LiNO_3$ + CH solution for 28 days at 80 °C, and analyzed by laser ablation inductively-coupled mass spectroscopy (LA-ICP-MS).

A portland cement with high alkali content (0.91% Na_2Oe) was used throughout the study. A commercial $LiNO_3$ solution (30% by mass) was used in the expansion tests. $LiNO_3$ pellets (USP grade) were used as the lithium source for other tests. NaOH pellets (USP grade) were used as the source of Na^+ and OH^- ions for all the tests. Calcium hydroxide powder was used as the calcium source.

3. Results

3.1. Expansion tests

Fig. 1 shows the expansion testing results for the two aggregates NB and NS. In the accelerated mortar bar tests, $LiNO_3$ was able to suppress the expansion of mortar bars with both aggregates provided it was used at a level of 100% of the standard dose (i.e. [Li]/[Na + K] = 0.74) both in the bars and in the solutions. When the dose in the solution was decreased to 50%, but was maintained at 100% in the bars, $LiNO_3$ delayed the expansion of mortars with both aggregates, but inevitably deleterious expansion was observed. The delay in the onset of expansion was significantly greater for the NB aggregate. In concrete microbar tests, when lithium in the bars and in the solutions was both at 100% dose, lithium worked well with NB, but not with NS. When the dose was decreased to 50% in the solutions, but still 100% in the bars, lithium could only mitigate the deleterious expansion for NB at early ages. In the standard concrete prism tests, lithium could suppress the deleterious expansion for NB at 100% Li dose but not at 75%. However, for the NS aggregate, lithium could not effectively prohibit the expansion even at double the standard dose (i.e. [Li]/[Na + K] = 1.48), or when oven-dried aggregate was pre-soaked with 30% $LiNO_3$ solution for 28 days prior to producing the concrete.

3.2. Silica dissolution tests

Fig. 2 shows the silica dissolution test results. It can be seen that the addition of $Ca(OH)_2$ significantly reduces the amounts of silica in solution, but this is probably a result of the precipitation of Ca–Si phases rather than reduced silica dissolution. The presence of lithium in solution reduced the amount of silica in solution and also the amount of sodium consumed indicating that lithium suppresses reaction between sodium and silica. What is surprising from this study is that results could not discriminate between the two aggregates.

3.3. Microstructural examinations

Fig. 3 shows the SEM images of the Vycor glass disks after immersion in different alkaline solutions for 28 days at 80 °C. Table 1 shows the EDS analysis for the glass disks immersed in different alkaline solutions. When it was immersed in 1 M NaOH solution (Fig. 3a), the glass surface showed a worm-like structure with etching sites, but no reaction product was found on the glass surface. EDS analyses of the glass surface showed that the glass compositions were very close to that of the starting material. With the addition of $Ca(OH)_2$ (Fig. 3b), the glass surface was etched and, again, no reaction product was found on the glass surface. EDS analyses revealed that the glass compositions were very close to that of the starting material as well. But there were some solid precipitates in the container. These precipitates were collected after taking the glass specimens out, and were then analyzed by XRD. The XRD spectra are shown in Fig. 4.

When immersed in 1 M NaOH + 0.74 M $LiNO_3$, as shown in Fig. 3c, the whole glass surface was completely covered by a very thick layer

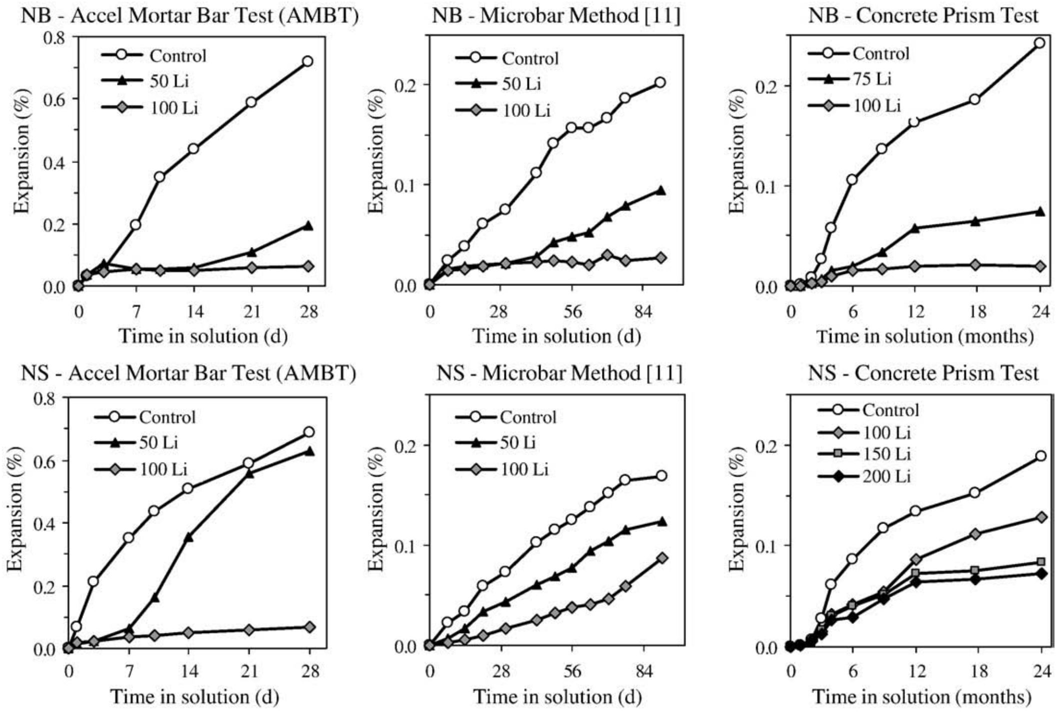

Fig. 1. Results from expansion tests (for AMBT and microbar test for 50 Li and 100 Li, the bars contained 100% of the standard lithium dose and the solution contained either 50% or 100% of the standard dose).

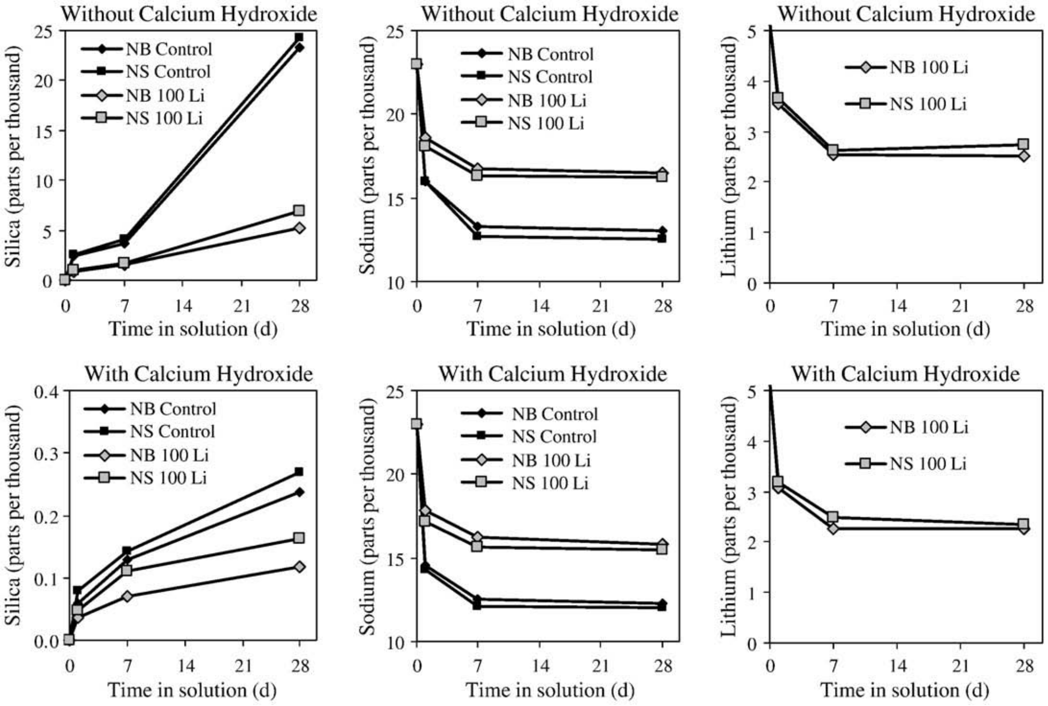

Fig. 2. Silica dissolution test results (note different scales).

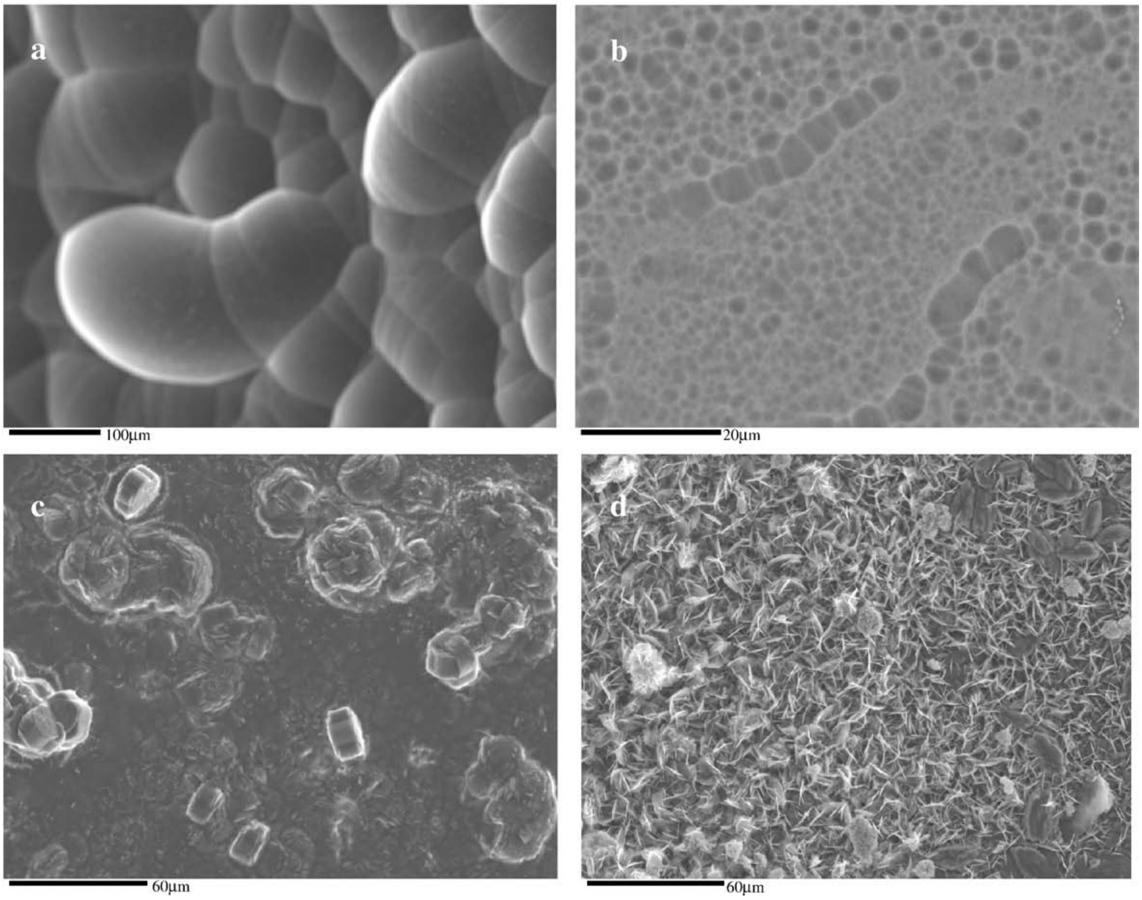

Fig. 3. SEM images of Vycor glass disks immersed in alkaline solutions for 28 days at 80 °C. (a) in 1 N NaOH, showing the globular structure with no reaction product (scale bar = 100 μm) ; (b) in 1 N NaOH + CH, showing the etching sites without reaction product (scale bar = 20 μm); (c) in 1 N NaOH + 0.74N $LiNO_3$, showing clusters of Li_2SiO_3 crystals (scale bar = 60 μm); (d) in 1 N NaOH + 0.74N $LiNO_3$ + CH, showing a matrix of ASR gel and Li_2SiO_3 crystals, or the ASR gel sitting on top of Li_2SiO_3 crystals (scale bar = 60 μm).

Table 1
EDS analysis (ZAF corrected) for Vycor glass disks immersed in alkaline solutions for 28 days at 80 °C.

Solution	#	Na_2O	Al_2O_3	SiO_2	K_2O	CaO	Total	C/S [a]
1 M NaOH	1	5.29	1.65	88.53	0.71	0.02	96.20	0.00
	2	4.63	1.71	82.46	0.85	0.09	89.74	0.00
	3	3.29	1.23	92.31	0.65	0.35	97.83	0.00
	4	4.24	1.38	90.56	0.54	0.21	96.93	0.00
	5	2.38	0.94	93.42	0.34	0.11	97.19	0.00
	6	1.95	0.77	88.47	0.28	0.14	91.61	0.00
	7	1.27	1.11	89.75	0.51	0.27	92.91	0.00
1 M NaOH + $Ca(OH)_2$	1	4.46	1.68	92.78	0.7	0.1	99.72	0.00
	2	4.89	1.62	92.02	0.61	0.07	99.21	0.00
	3	4.28	0.49	87.34	0.04	0.56	92.71	0.01
	4	3.92	1.29	91.23	0.14	0.34	96.92	0.00
	5	4.6	1.43	89.43	0.45	0.85	96.76	0.01
	6	2.39	0.93	90.45	0.23	0.77	94.77	0.01
	7	3.88	1.07	89.67	0.09	0.69	95.40	0.01
1 M NaOH + 0.74 M $LiNO_3$	1	0.85	0.63	68.71	0.06	0.16	70.41	0.00
	2	0.69	0.94	71.97	0.05	0.09	73.74	0.00
	3	0.47	0.7	67.47	0.03	0.16	68.83	0.00
	4	0.23	0.39	64.09	0.23	0.31	65.25	0.01
	5	0.18	0.45	65.34	0.36	0.05	66.38	0.00
1 M NaOH + 0.74 M $LiNO_3$ + $Ca(OH)_2$	1	1.39	2.48	70.05	0.05	0.37	74.34	0.01
	2	0.58	0.71	68.86	0.04	0.28	70.47	0.00
	3	1.08	1.29	63.89	0.91	0.44	67.61	0.01
	4	0.54	2.04	66.32	0.33	0.56	69.79	0.01
	5	3.47	0.92	38.31	0.26	6.53	49.49	0.18
	6	2.38	1.06	40.06	0.17	6.39	50.06	0.17
	7	9.4	3.62	42.83	0	5.23	61.08	0.13
	8	9.19	1.13	34.94	0.05	4.63	49.94	0.14
	9	4.73	0.75	40.94	0.12	4.61	51.15	0.12
	10	5.47	0.57	38.35	0.13	1.92	46.44	0.05

[a] Ca/Si Molar ratio.

of crystalline material with 64–72% SiO_2 by mass from the EDS analyses. Before carbon coating for SEM examinations, the same piece disk was examined using XRD analysis and it was confirmed that this crystalline deposit was Li_2SiO_3.

With the addition of CH (Fig. 3d), the glass surface was covered by a matrix of white rosette crystalline ASR gel products and darker crystalline phases with 64–70% SiO_2 which might be Li_2SiO_3 crystals. The ASR gel had a CaO content of 2–7% by mass with a calcium-to-silicon molar ratio of C/S = 0.05–0.20. These gels may contain certain amounts of lithium, but due to limitations of EDS, no information about the lithium content could be obtained.

Fig. 4 shows the XRD results for the solid residues obtained from glass immersion tests. When immersed in NaOH solution, the solution was clear, and no solid residue was found, suggesting that silica dissolves but no new solid phase forms (i.e. the silica remains in solution). The residues that were collected from the solution of NaOH with CH, a crystalline phase was identified as $Ca_{4.5}Si_6O_{15}(OH)_3 \cdot 2H_2O$. For the residue obtained from solution containing 1 N NaOH and 0.74 M $LiNO_3$, Li_2SiO_3 was found. With both $LiNO_3$ and CH in solution, interestingly, only CH was left in the solution, which means both the Li_2SiO_3 and gel products seen on the glass surface by SEM (Fig. 3d) were strongly bound at the glass surface rather than producing residue in the containers.

Fig. 5 shows the elemental distributions from LA-ICP-MS across the interface of a Vycor glass disk-cement paste specimen. It can be seen that at the glass surface area, there is a layer which is very rich in Li and Si, which may correspond to the Li_2SiO_3 crystalline phase observed by SEM and XRD, or the presence of a thin layer of lithium-bearing alkali–silica gel.

Fig. 6 shows the SEM images for polished NB disks immersed in different alkaline solutions for 28 days at 80 °C. When immersed in 1 M NaOH (Fig. 6a), the disk surface was covered by a layer of reaction products. It was hard to discern the morphology of these products. EDS analyses revealed that their compositions were very variable but generally were high in Ca. With the addition of CH (Fig. 6b), a gel product covered the entire disk surface. This gel contained a very high amount of Ca with a C/S of 0.51–0.87. In the presence of 0.74 M $LiNO_3$ (Fig. 6c), some areas were covered by large Li_2SiO_3 particles with a palm-like morphology (top left of image), no significant gel product was found. With the addition of CH (Fig. 6d), a matrix of large Li_2SiO_3 crystal particles and white gel covered the entire surface. The gel was found to contain a much lower amount of Ca with a C/S of 0.01–0.19.

Fig. 7 shows the SEM images for polished NS disks immersed in different alkaline solutions for 28 days at 80 °C. When immersed in 1 M NaOH (Fig. 7a), a gel reaction product was found with variable Ca content that gave a C/S of 0.31–1.28. With the addition of CH (Fig. 7b), more gel products were found to spread out over the entire disk surface, these gels also contained very high amounts of Ca with a C/S of 0.22–0.86. In the presence of 0.74 M $LiNO_3$ (Fig. 7c), small Li_2SiO_3 crystals were found at the surface but were not enough to cover the entire surface. With the addition of CH (Fig. 7d), the small hexagonal Li_2SiO_3 crystal particles were accumulated at some locations and formed a matrix with ASR gels. Unlike the Li_2SiO_3 crystals found in NB immersion specimens, most crystals formed here were small in size and the gels that formed here contained a wide range of Ca with a C/S varying from 0 to 0.68.

Li, Ca, and Si distributions were also determined by LA-ICP-MS for the cement–aggregate interface for the cement–aggregate specimens with NB and NS. Unlike the glass immersion tests shown in Fig. 5, no significant Li-rich layer was found at the interface between the aggregate particle and cement paste, but there was a significant amount of Li detected within the aggregate particles, especially for the

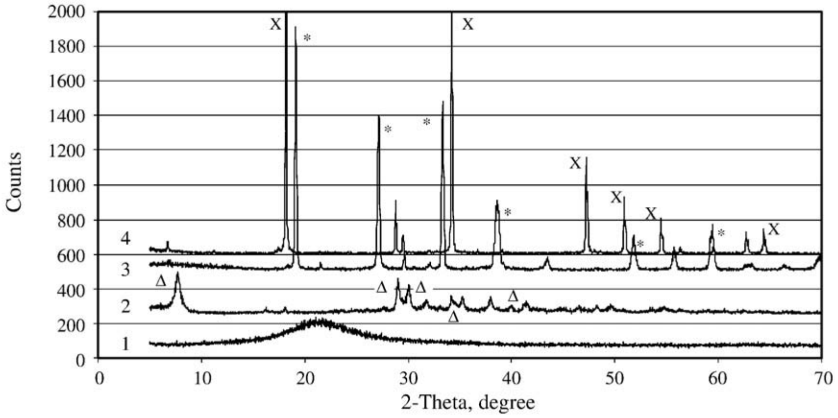

Fig. 4. XRD spectra for the solid residues obtained from the glass immersion tests. 1) Starting glass powder; 2) in 1 N NaOH + CH; 3) in 1 N NaOH + 0.74N $LiNO_3$; 4) in 1 N NaOH + 0.74 N $LiNO_3$ + CH. X portlandite, * Li_2SiO_3, Δ $Ca_{4.5}Si_6O_{15}(OH)_3 \cdot 2H_2O$.

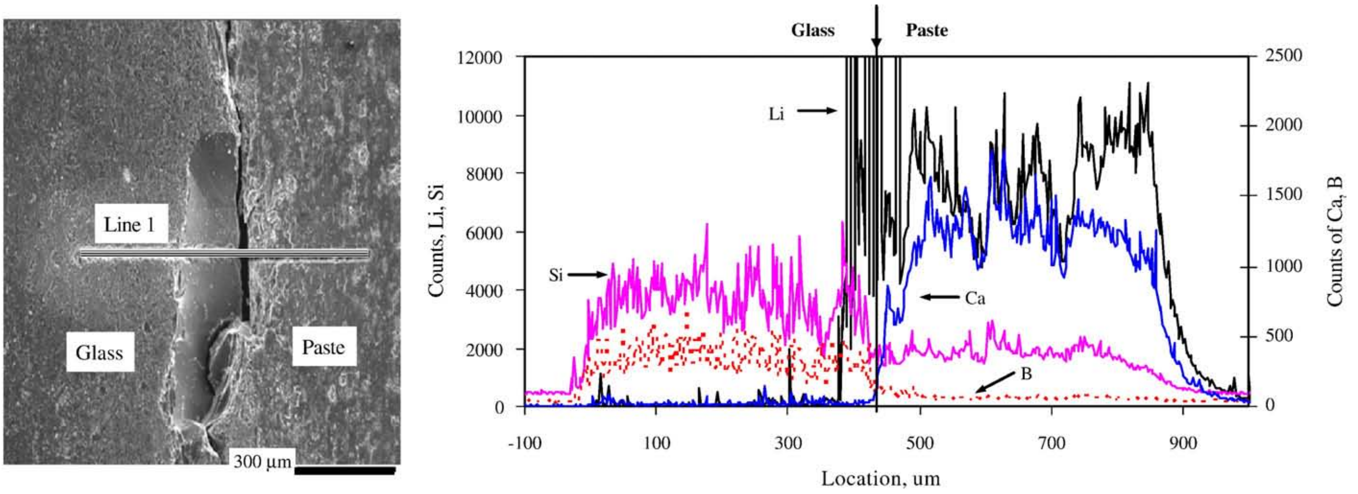

Fig. 5. Elemental distributions of the glass disk-cement paste specimens.

NB aggregate. These lithium ions may exist in the solution, as Li_2SiO_3 crystals and Li-bearing ASR gels, or may be a constituent of the aggregate.

4. Discussions

Based on the above findings, a mechanism for the suppressive effect of $LiNO_3$ in controlling ASR expansion can be proposed: the formation of Li_2SiO_3 crystals and Li-bearing, low Ca ASR gel was responsible for the inhibiting behavior of $LiNO_3$ against ASR. These two phases either form a matrix that could completely cover the entire reactive silica particle surface, or the Li_2SiO_3 serves as a base with the Li-bearing, low Ca gel sitting on top of the crystals. The Li-bearing, low Ca gel was different from conventional ASR gel. It was very stable, with little or no mobility, thus having a strong binding with the reactive silica particle. If sufficient amounts of Li_2SiO_3 crystal and Li-bearing, low Ca gel form it is possible that the reactive silica particle surface might be completely covered, providing a

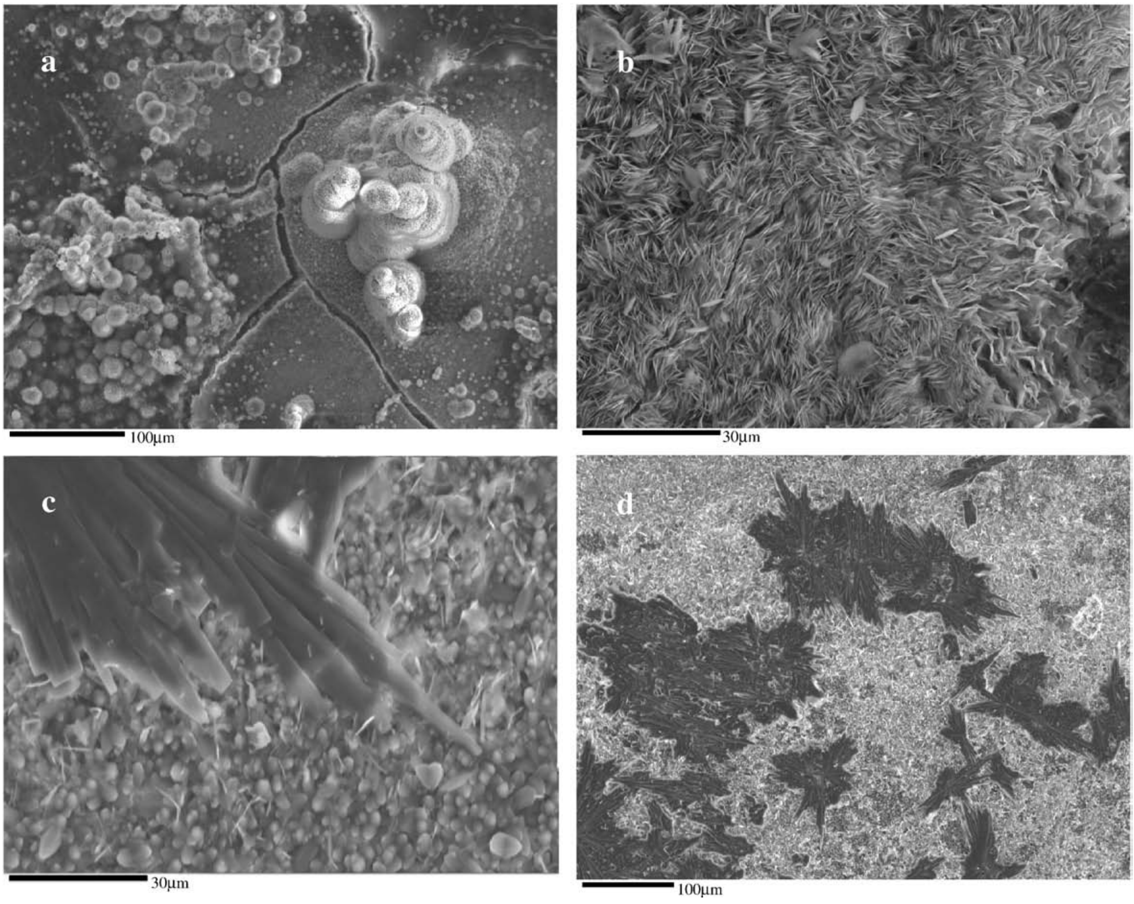

Fig. 6. SEM images of NB polished disks immersed in alkaline solutions for 28 days at 80 °C (a) in 1 N NaOH, showing a layer of reaction products (scale bar = 100 µm); (b) in 1 N NaOH + CH, showing the gels with a C/S of 0.51–0.87 (scale bar = 30 µm); (c) in 1 N NaOH + 0.74 N $LiNO_3$, showing large Li_2SiO_3 crystals with no significant ASR gel product (scale bar = 20 µm); and (d) in 1N NaOH + 0.74 N $LiNO_3$ + CH, showing a matrix of Li_2SiO_3 crystals and ASR gel with a C/S of 0.01–0.19 (scale bar = 100 µm).

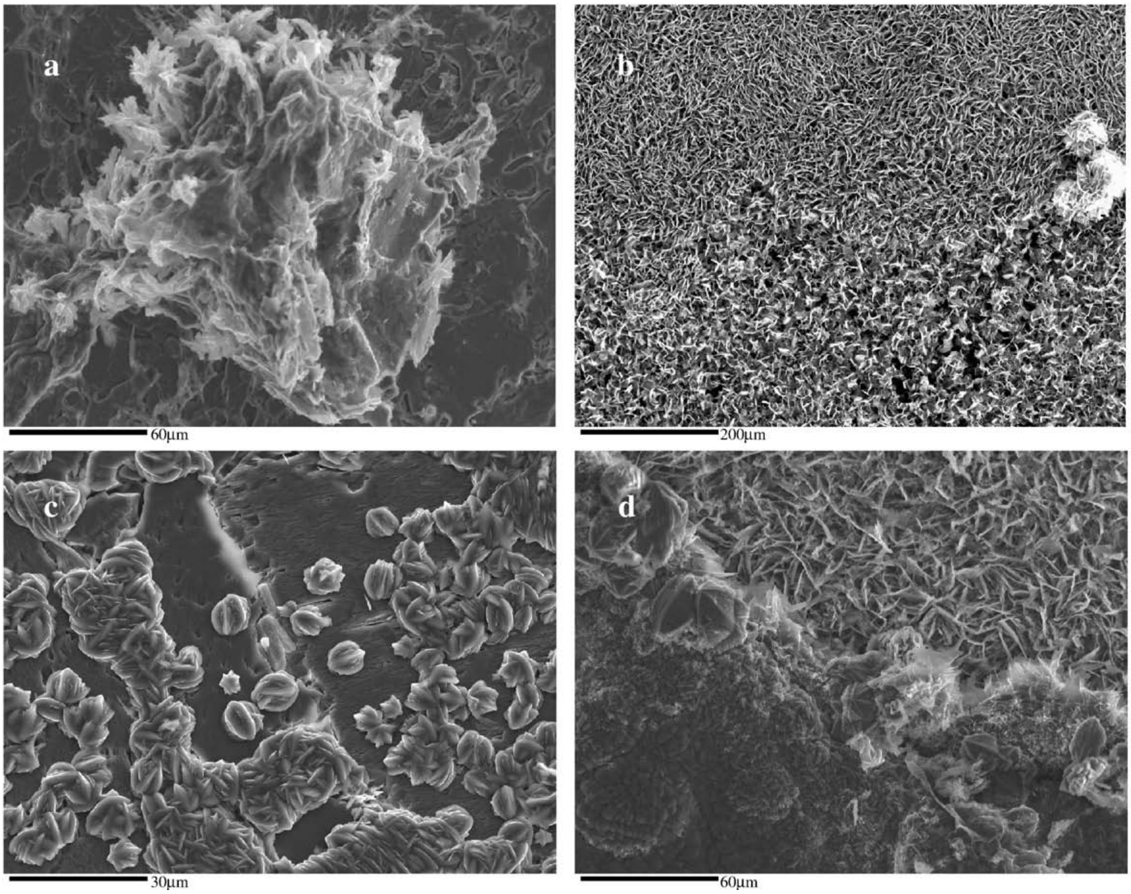

Fig. 7. SEM images of NS polished disks immersed in alkaline solutions for 28 days at 80 °C. (a) in 1 N NaOH, showing a gel products with a C/S of 0.31–1.38; (b) in 1 N NaOH + CH, showing the gels with a C/S of 0.22–0.86; (c) in 1 N $NaOH + 0.74$ N $LiNO_3$, showing small accumulated Li_2SiO_3 crystals with no significant ASR gel product; (d) in 1 N $NaOH + 0.74$ N $LiNO_3 + CH$, showing a matrix of Li_2SiO_3 crystals and ASR gel with a C/S of 0–0.68.

diffusion barrier that prevents further penetration of hydroxyl ions which stifles the continued dissolution of silica from the aggregate surface.

As shown below, the types of ASR reaction products depend on the CaO content and the Li content in mixture.

$$Li_2SiO_3 \rightarrow Li-(\text{low Ca})-Na-Si\ \text{gel} \rightarrow Li-(\text{high Ca})-Na-Si\ \text{gel} \rightarrow Ca-Na-Si\ \text{gel}$$

$$\text{CaO\%:}\ 0 \longrightarrow \text{high}$$

$$\text{Li\%:}\ 100 \longrightarrow 0$$

Li_2SiO_3 and Ca–Na–Si gel are the two end members of the reaction products. Conventionally in the absence of Li, the ASR gel will absorb more Ca with time, and gradually Ca may replace alkalis in the reaction product, thereby regenerating alkalis for further reaction [12,13]. It is possible that in the presence of lithium, the ASR reaction products, such as Li_2SiO_3 and Li–(low Ca)–Na–Si gel, have a denser and more stable structure. These rigid products have a stronger bond with the reactive SiO_2 particles, and have lower mobility to disperse within cement paste to absorb additional Ca. Hence, the alkali recycling process in which Na and K are replaced by Ca may not occur. These reaction products may also have lower capacity to imbibe moisture from the surrounding environment to cause cracking. Here a threshold C/S ratio for these non-expansive gels may be proposed as 0.2, because gels with a C/S below 0.2 were usually observed in immersion samples with 100% lithium dose and within aggregate particles in concrete specimens. Gels with higher C/S were mostly found in samples without lithium, samples with 50% lithium addition, and in NS immersion and concrete specimens where the expansion tests showed that NS did not respond well to $LiNO_3$. Indeed, the gels formed in the samples with 50% lithium might contain very low or no lithium at all. Apparently no extra lithium was available to participate in the gel formation because the C/S ratio of these gels is within the same range as that of the control samples and the Li_2SiO_3 was found without a good morphology, which means there was insufficient lithium to keep up with the formation of this crystal.

Moreover, the current results did show that calcium does play a very important role in the formation of ASR gel products. In the glass immersion tests with NaOH and $LiNO_3$ solution, no gel was observed. Without calcium ions, the residual solution is merely an alkali–silica solution. Thus calcium ions initiate the condensation of silicate ions in solution and link the silicate species in order to form a solid [14]. Therefore, the presence of calcium is essential for the formation of ASR gel and thus the expansion due to ASR.

The different responses of NB and NS aggregates to LiOH can be attributed to the difference in their textural structures. As shown in Fig. 8, NB is coarse grained, and the surface of reactive silica particles will be exposed immediately to the pore solution of concrete or mortar and will thus have equal access to both sodium and lithium alkalis. This permits the protective lithium–silica (Li–Si) barrier to form at the surface and “protect” the underlying silica from attack by sodium (or potassium) hydroxides. NS is fine grained with reactive microcrystalline or strained quartz being embedded in a dense non-reactive matrix. The reactive aggregate does not have immediate access to lithium when the mortar or concrete is first mixed and there

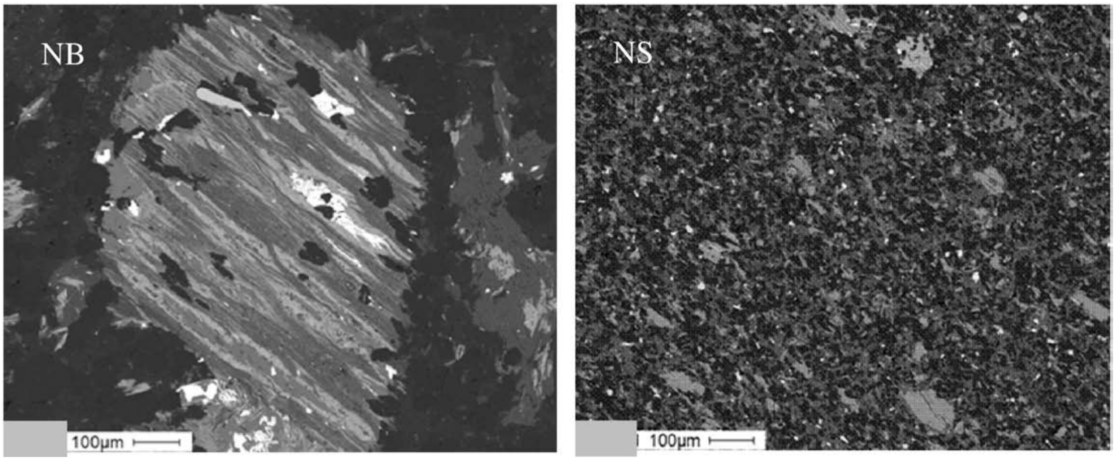

Fig. 8. Aggregate microstructure by SEM.

will be a competition between the Na (K), Li and OH ions to reach the reactive silica. Given the large hydrated radius of the lithium ion, it is probable that sodium (and potassium) hydroxides reach these sites before lithium and deleterious alkali–silica reaction is not prevented.

In the mortar bar test and the silica dissolution test, the coarse aggregate particles were crushed (below 5 mm or smaller), and this likely increases the accessibility of the reactive silica and, thus, the efficacy of the lithium in preventing damaging reaction. In the concrete prism and microbar test, where larger aggregate sizes are used, the lithium is found to be less effective with the NS aggregate because its reactive silica has less access to the lithium.

5. Concluding remarks

Based on the data presented in this paper, the following hypotheses are put forward:

1. The suppressive effect of $LiNO_3$ against ASR may be attributed to the formation of Li_2SiO_3 crystal and Li-bearing, low Ca gel, which could serve as the protection layer to prevent the reactive silica from further attack by hydroxyl ions.
2. $LiNO_3$ could completely inhibit the deleterious expansion in the accelerated mortar bar tests for both NB and NS aggregates provided that the Li doses were controlled at 100% of the standard dose both in the bars and in the soaking solutions. But in the concrete prism tests and concrete microbar tests which used larger reactive aggregate particles, $LiNO_3$ could only mitigate the deleterious expansion for the NB aggregate but not for the NS aggregate.
3. The different responses of $LiNO_3$ to NB and NS aggregates in concrete expansion tests was ascribed to their different textural features, the reactive silica in the NS aggregate being less accessible than in the NB aggregate.

Further studies are underway to test these hypotheses.

References

[1] E.J. McCoy, A.G. Caldwell, New approach to inhibiting alkali-aggregate expansion, Journal of the American Concrete Institute 22 (1951) 693.

[2] M. Lawrence, H.F. Vivian, The reactions of various alkalis with silica, Australian Journal of Applied Science 12 (1961) 96.

[3] Y. Ohama, K. Demura, M. Kakegawa, Inhibiting alkali-aggregate reaction with chemical admixtures, 8th International Conference on AAR in Concrete, Kyoto, Japan, 1989, pp. 253–258.

[4] Y. Sakaguchi, M. Takakura, A. Kitagawa, T. Hori, F. Tomosawa, M. Abe, The inhibiting effect of lithium compounds on ASR, 8th International Conference on AAR in Concrete, Kyoto, Japan, 1989, pp. 229–234.

[5] D. Stark, Lithium salt admixtures — an alternative method to prevent expansive alkali–silica reactivity, 9th International Conference on AAR in Concrete, London, UK, 1992, pp. 1017–1025.

[6] D. Stark, B. Morgan, P. Okamoto, S. Diamond, Eliminating or minimizing the risk of alkali–silica reactivity, National Research Council, Strategic Highway Research Program (SHRP), SHRP-C 343, Washington D.C., 1993 266 pp.

[7] K. Folliard, M.D.A. Thomas, B. Fournier, K. Kurtis, J. Ideker, Interim Recommendations for the Use of Lithium to Mitigate or Prevent ASR, , 2006 Publication No. FHWQ-HRT-06-073.

[8] S. Diamond, Unique response of $LiNO_3$ as an alkali silica reaction-preventive admixture, Cement and Concrete Research 29 (8) (1999) 1271–1275.

[9] D.B. Stokes, H.H. Wang, S. Diamond, A lithium-based admixture for ASR control that does not increase the pore solution pH, 5th CANMET/ACI International Conference on Superplastisizers and Other Chemical Admixtures in Concrete, Roma, Italy, ACI SP 173, 1997, pp. 855–868.

[10] X. Feng, M.D.A. Thomas, T.W. Bremner, B.J. Balcom, K.J. Folliard, Studies on lithium salts to mitigate ASR-induced expansion in new concrete: a critical review, Cement and Concrete Research 35 (9) (2005) 1789–1796.

[11] P.E. Grattan-Bellew, Cybanski George, B. Fournier, L. Mitchell, Proposed Universal Accelerated Test for Alkali-aggregate Reaction: the Concrete Microbar Test, 2003 NRCC-46876.

[12] W.C. Hansen, Studies relating to the mechanism by which alkali-aggregate reaction produces expansion in concrete, Journal of the American Concrete Institute Proceedings 40 (3) (1944) 213–227.

[13] M.D.A. Thomas, The role of calcium hydroxide in alkali recycling in concrete, Calcium Hydroxide in Concrete, Mater. Sci. Concr, 2001, pp. 225–236.

[14] P. Nieto, H. Zanni, Polymerization of alkaline–calcium–silicate hydrates obtained by interaction between alkali–silica solutions and calcium compounds. A ^{29}Si nuclear magnetic resonance study, Journal of Materials Science 32 (13) (1997) 3419–3425.